

Toward an Understanding of the Anisotropy in Hcp Zinc Metal: Total Scattering Structural Study Using Synchrotron-Based, Temperature-Dependent, X-Ray Pair Distribution Function Analysis

Ahmad S. Masadeh^a, Gassem M. Alzoubi^b, Moneeb T. M. Shatnawi^a,
Osama Abu-Haija^c, Ziad Abu Waar^a and Yang Ren^d

^a Department of Physics, The University of Jordan, Amman 11942, Jordan.

^b Department of Physics, Faculty of Science, The Hashemite University, Zarqa 13133, Jordan.

^c Applied Physics Department, Tafila Technical University, P. O. Box 179, Zip Code 66110, Tafila, Jordan.

^d X-Ray Science Division, Advanced Photon Source, Argonne National Laboratory, Argonne, Illinois 60439, USA.

Doi: <https://doi.org/10.47011/17.1.2>

Received on: 24/11/2021;

Accepted on: 28/08/2022

Abstract: Among hexagonal close packing (hcp) metals, zinc has a non-ideal hcp structure due to a significantly increased axial ratio c/a . We studied the behavior of the ratio of lattice constants c/a and the ratio of thermal displacement parameters (U_{33} / U_{11}) in the temperature range of 100-300 K, using the X-ray total scattering atomic pair distribution function (PDF) analysis over different refinement r -ranges. The temperature-dependent PDF analysis confirmed that the crystal structure of zinc has significant static distortion along the c -direction. The measured value of atomic displacement parameters of zinc showed a notable anisotropy as expressed by the ratio U_{33} / U_{11} of ≈ 2.2 at 100 K. The lattice parameter ratio c/a was slightly reduced at low temperatures but remained unusually large. The extrapolated value of the ratio c/a reached 1.832 at 0 K. The PDF refinements using the crystallographic model revealed that there are some local structure features in zinc that are not captured by the crystallographic model. On the other hand, our local structure refinement indicated a presence of local bond distortion along the z -direction that averaged out over wider r -range refinements with a large U_{33} value.

Keywords: Hcp anisotropy, Zinc metal, Total scattering, X-ray scattering, Pair distribution function.

PACs numbers: 61.46.Df, 61.10.-i, 78.66.Hf, 61.46.-w.

1. Introduction

The crystal structure of the Zn element deviates from the ideal hcp structure due to a significantly increased axial ratio c/a . A more intriguing challenge arises when attempting to understand what prevents the Zn atoms from moving into the ideal hcp structure. The reason

why zinc exhibits a structurally unusual c/a ratio is not completely understood until now. The crystal structure of Zn was investigated as a function of temperature, ranging from 40 to 500 K, using single-crystal X-ray diffraction by Nuss *et al.* [1]. They reported that the thermal motion

of Zn shows a striking anisotropy as expressed by a ratio U_{33} / U_{11} of ≈ 2.6 at 500 K [1]. The electronic origin of the structural anomalies of zinc was studied by Wedig *et al.* using experimental and theoretical calculations [2]. Their findings indicated that the anomalies of c/a ratio are caused by $4s-3d$ electron interactions rather than anisotropy in thermal expansion, and they suggested that the anomalous hcp structure of zinc results from a kinetic balancing of the valence electrons, i.e. through correlation-mediated $4s-3d$ interactions [2].

Most of the previous crystal structure studies done on Zn metal employed conventional X-ray diffraction (XRD) methods to study its atomic structure. Conventional XRD experiments probe into the presence of a periodic structure, i.e. long-range order, which is reflected in the Bragg peaks. Conversely, local structural deviations, i.e. short-range order features, mainly affect the diffuse scattering intensity. To obtain information about both long and short-range orders, a technique that takes into consideration both the Bragg and the diffuse scattering intensities needs to be used. The total scattering atomic pair distribution function (PDF) technique is one such approach. The atomic PDF analysis is a powerful method for studying the structure of locally distorted materials [3, 4].

In this work, we have applied a non-traditional approach, the X-ray total scattering atomic PDF technique, to study the temperature dependence of lattice constants and thermal motion parameters of Zn metal at different atomic length scales.

2. Experimental Details

2.1 Data Collection

The temperature-dependent PDF experiment was performed at the 11-ID-C beamline of the Advanced Photon Source (APS) at the Argonne National Laboratory, Lemont, IL (USA). The powder sample (Zn) was packed in a Kapton capillary with a 1.0 mm diameter and measured in transmission geometry in the temperature range of 100-300 K. Data were collected using RAPDF [5] experiment setup with x-ray energy of 114.8 keV ($\lambda = 0.1080$ Å). The two-dimensional (2D) raw data were integrated and converted to intensity versus 2θ , where 2θ is the angle between the incident and scattered x-rays, using the software Fit2D [6].

The PDFgetX3 software [7] was used to correct the converted intensity $I(2\theta)$ using standard methods [3, 4, 8, 9] to obtain the total scattering structure function, $S(Q)$, where the value of the momentum transfer (Q) is given by $Q = \frac{4\pi}{\lambda} \sin\theta$. Then the $S(Q)$ data were processed to obtain the experimental reduced total scattering structure function, $F(Q)$, and experimental PDF, $G(r)$ [3].

In the Fourier transform step, to obtain the PDF, $G(r)$, from $S(Q)$, the data are truncated at a finite maximum value of the momentum transfer, denoted as Q_{max} . Here, $Q_{max} = 35.0$ Å⁻¹ was found to be optimal. Different values of Q_{max} can be considered during the Fourier transform step. The value of Q_{max} is optimized to reasonably minimize the introduced noise level, as the signal-to-noise ratio decreases with increasing Q value. More details about the image plate (IP) data corrections are described in earlier work by Masadeh *et al.* [10]. Additionally, area detector corrections for high-quality synchrotron X-ray structure factor measurements were discussed by Skinner *et al.* [11].

The PDF is a powerful local structural technique that yields quantitative structural information at different length scales using X-ray and neutron powder diffraction data [3, 4]. Recent developments in both data collection [5, 10, 12, 13] and modeling [7, 14-17] have enhanced the potential of this technique for quantitatively determining the structure of complex materials. Successful applications of the PDF method have been demonstrated in previous studies [18-21]. This study employs the X-ray total scattering PDF method to investigate the crystal structure of Zn metal within the temperature range of 100 to 300 K for different refinement ranges: long-range refinement (LRR) for the fitting range of 2-35 Å and short-range refinement (SRR) for the fitting range of 2-10 Å.

3. Results and Discussion

The XRD data for zinc metal are collected for a wide range of momentum transfer (Q) in the temperature range of 100 to 300 K. The experimental reduced structure function, $F(Q)$, for selected temperatures, is shown in Fig. 1. As can be seen from this figure, the $F(Q)$ pattern shows a significant intensity up to the highest

values of Q , highlighting the value of measured data over such a wide Q range in the reciprocal space. On the other hand, in the real space, the

corresponding PDFs, $G(r)$, are shown in Fig. 2, where high-quality PDFs are obtained, with a high Q_{max} value of 35.0 \AA^{-1} .

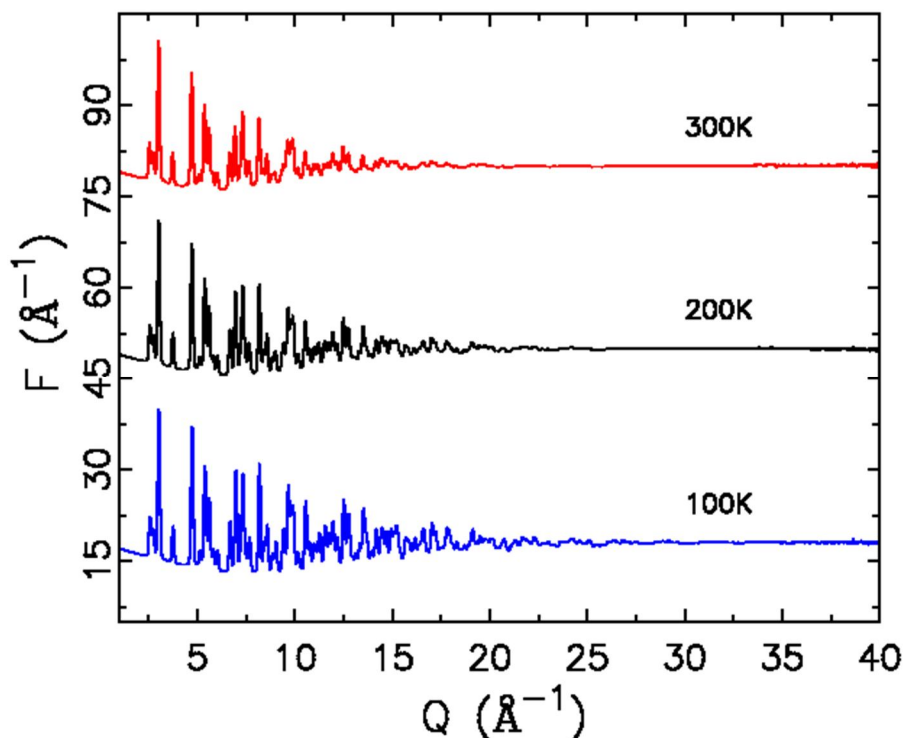


FIG. 1. The experimental reduced structure function $F(Q)=Q*(S(Q)-1)$ for Zn at different selected temperatures.

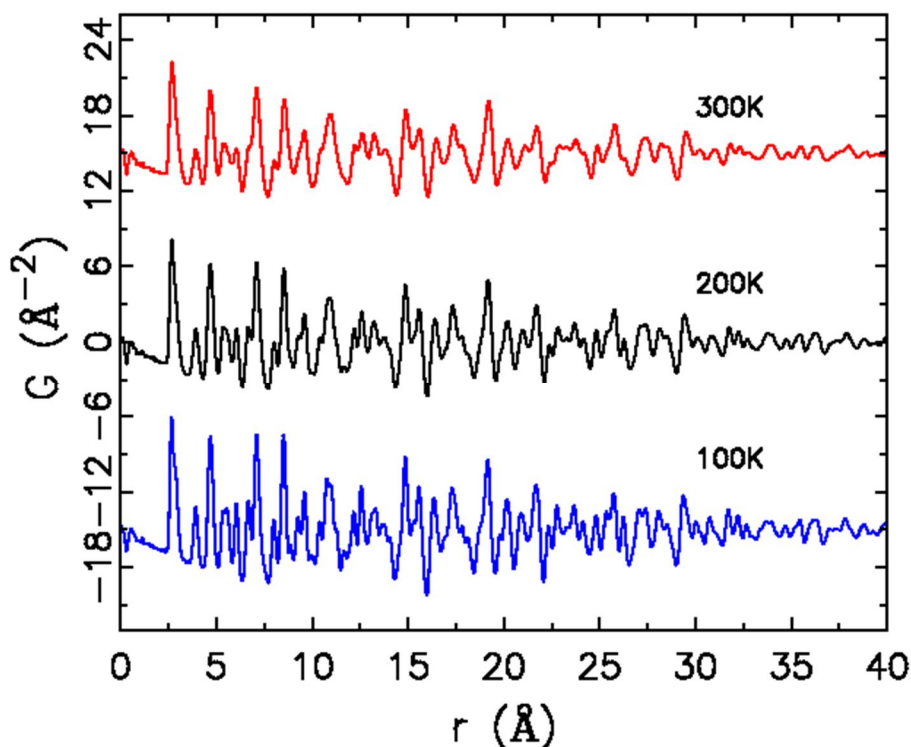


FIG. 2. The experimental atomic pair distribution function, $G(r)$, obtained by Fourier transforming the data in Fig. 1.

The PDF method is a direct space probe that uses both Bragg and diffuse scattering intensities

to provide structural information at different length scales: short, long, and intermediate-range

orders. The zinc metal has a well-known hexagonal crystal structure, where the zinc atom is located at the special Wyckoff position $2c$ ($1/3, 2/3, 1/4$) in space group $P6_3/mmc$ (No. 194). Therefore, its static structural property is determined by four variable parameters; namely, the lattice constants a and c , as well as the coefficients of thermal motion U_{11} and U_{33} .

One structural model, hexagonal structure (space group $P6_3/mmc$), was considered for this PDF study. During the PDF refinement, the lattice constants, scale factor, and anisotropic thermal factors were refined, with all parameters maintaining the symmetry of the hexagonal structure. The crystal structure of zinc metal was studied in the temperature range of 100-300 K. The results of the full-profile fitting to the PDF data for the fitting range of $2\text{-}35 \text{ \AA} \equiv (\text{LRR})$ are shown in Fig. 3 and the obtained structural parameters are listed in Table 1.

Our results show that the used hexagonal model fits the PDF data very well with an excellent agreement factor (R_w) value of 0.04 for a maximum refinement range of 35.0 \AA . The PDF results show a striking anisotropy in the thermal motion of zinc at room temperature. The values of the atomic displacement parameter (ADP) along the c -direction (U_{33}) are found to be almost three times larger compared with the values of the ADPs in the basal plane ($U_{11} = U_{22}$), as the ratio of U_{33} / U_{11} is found to be about 2.5, which confirms the result obtained earlier by Masadeh *et al.* [22]. This result also agrees with the ratio of the mean square amplitudes along the principal axes measured by Merisalo *et al.* [23] using elastic thermal-neutron scattering data at 295 K. They obtained a ratio of 2.55 for harmonic model 1, 2.25 for anharmonic model 1, and 2.30 for anharmonic model 2, as published in Table 3 by Merisalo *et al.* [23].

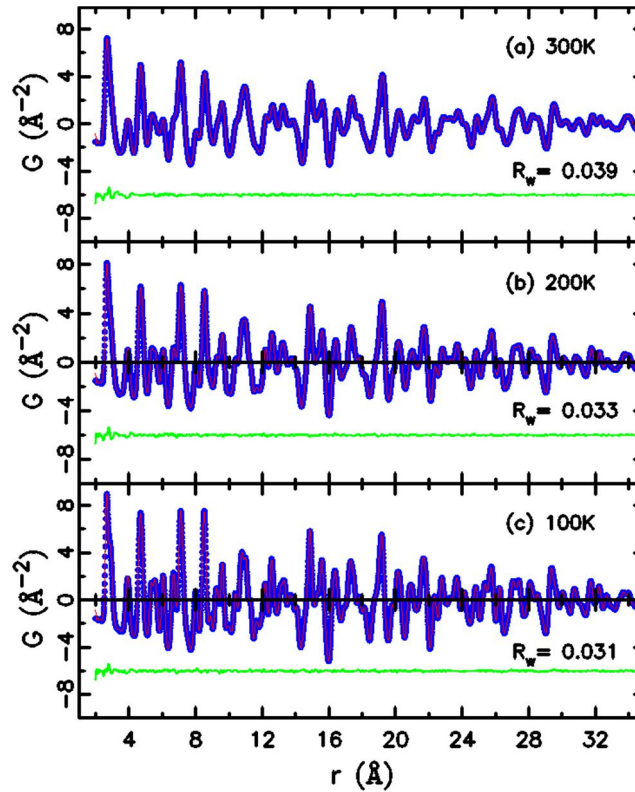


FIG. 3. Long-range refinement with r -range from 2 to 35 \AA : The experimental PDF, $G(r)$, (solid dots) and the calculated PDF from the refined structural model (solid line). The difference curve is shown offset below.

To shed some light on local structure features, we have performed short-range PDF refinement for a fitting range from 2 to $10 \text{ \AA} \equiv (\text{SRR})$ based on the well-known hexagonal model. The resulting fit is shown in Fig. 4. The difference curve in this figure shows that the position of the first out-of-plane bond ($r =$

2.9120 \AA) appears to be not captured locally. Based on the used hexagonal model and by looking at the difference curve that is shown offset below in Fig. 4, the N-shaped feature (\sim) centered at $r = 2.9120 \text{ \AA}$ indicates that the position of the first out-of-plane bond ($r = 2.9120 \text{ \AA}$) tends to be shorter locally.

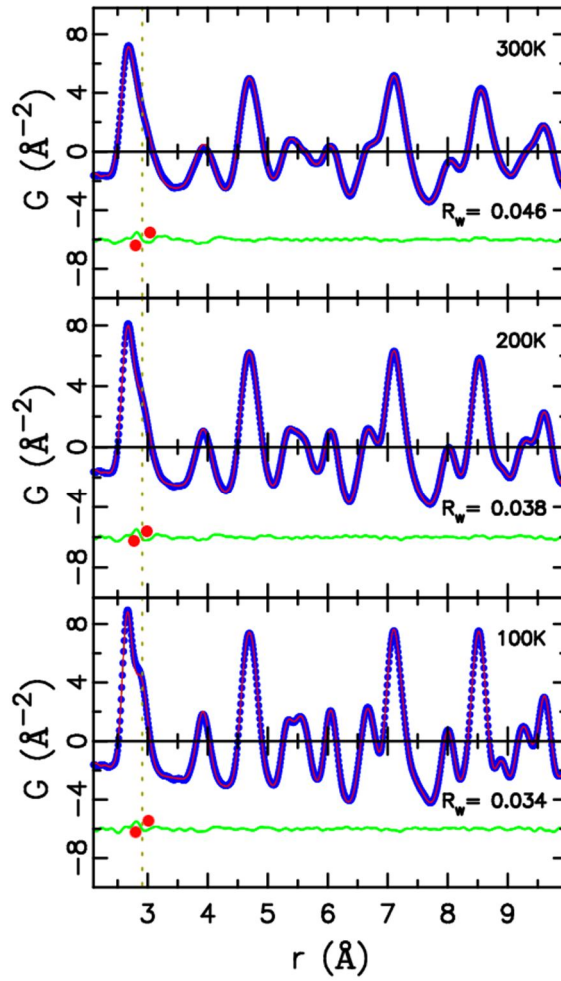


FIG. 4. Short-range refinement with r -range from 2 to 10 Å. The experimental PDF, $G(r)$, is represented by solid dots. The calculated PDF from the refined structural model is shown as a solid line. The difference curve is shown offset below the N-shaped feature (\sim) centered at $r = 2.9120$ Å, indicating that the position of the first out-of-plane bond (2.9120 Å) appears to be shorter locally. The vertical dashed line and the red dots are guides to the eye.

TABLE 1. The refined parameter values obtained from PDF refinement for Zn metal measured in the temperature range of 100 to 300 K with r -range from 2 to 35 Å. The lattice constants and the anisotropic displacement parameters (U_{ij}) are refined assuming the hcp structure, space group $P6_3/mmc$, ($U_{11} = U_{22} \neq U_{33}$).

T (K)	$a = b$ (Å)	c (Å)	U_{11} (Å ²)	U_{33} (Å ²)
300	2.6644(1)	4.9432(1)	0.01195(1)	0.02956(1)
280	2.6639(1)	4.9372(1)	0.01117(1)	0.02776(1)
260	2.6632(1)	4.9318(1)	0.01028(1)	0.02555(1)
240	2.6625(1)	4.9264(1)	0.00955(1)	0.02342(1)
220	2.6619(1)	4.9209(1)	0.00872(1)	0.02123(1)
200	2.6611(1)	4.9156(1)	0.00803(1)	0.01916(7)
180	2.6606(1)	4.9098(1)	0.00727(1)	0.01735(1)
160	2.6599(1)	4.9048(1)	0.00661(1)	0.01558(1)
140	2.6595(1)	4.9002(1)	0.00606(1)	0.01395(1)
120	2.6589(1)	4.8960(1)	0.00554(1)	0.01250(1)
100	2.5881(1)	4.8952(1)	0.00555(1)	0.01243(1)

3.1 Temperature Dependence of the Atomic Displacement Parameters

Using the well-known hexagonal model, the PDF data are fitted in the temperature range of 100 to 300 K with an LRR scale. The obtained structural parameters for low-temperature data are listed in Table 1. As can be seen, the obtained values of the ADPs (U_{11} and U_{33}) increase with temperature. This is expected, as the thermal motion exhibits reduced amplitude at low temperatures. We also investigated the thermal motion anisotropy, which is demonstrated by the U_{33} / U_{11} ratio as a function of temperature (Fig. 5). As the temperature reduces down to 100 K, the thermal anisotropy is expected to be less. This is clearly shown in Fig. 5, which displays the values of the ratio U_{33} / U_{11} in the temperature range of 300 to 100 K. This figure shows a reduction of the ratio U_{33} / U_{11} with reducing the temperature

value and indicates that the obtained ADP values (Table 1) along the c -direction (U_{33}) are still large compared to the values of the ADP in the ab plane ($U_{11} = U_{22}$), where the ratio U_{33} / U_{11} is found to be about 2.2 at 100 K. This result supports the presence of significant static distortion along the c -direction, the direction perpendicular to the basal plane. To study the local order features, we performed short-length scale refinements by fitting the PDF data using the SRR scale (2-10 Å). The resulting fit is shown in Fig. 4. The structural parameters obtained from the SRR scale were then compared to those obtained from the LRR scale. As depicted in Fig. 5, the SRR results reveal that the U_{33} parameter tends to have values similar to those obtained from the LRR scale as the temperature decreases, until the U_{33} / U_{11} ratio approaches its average value (2.2) at a temperature of 100K.

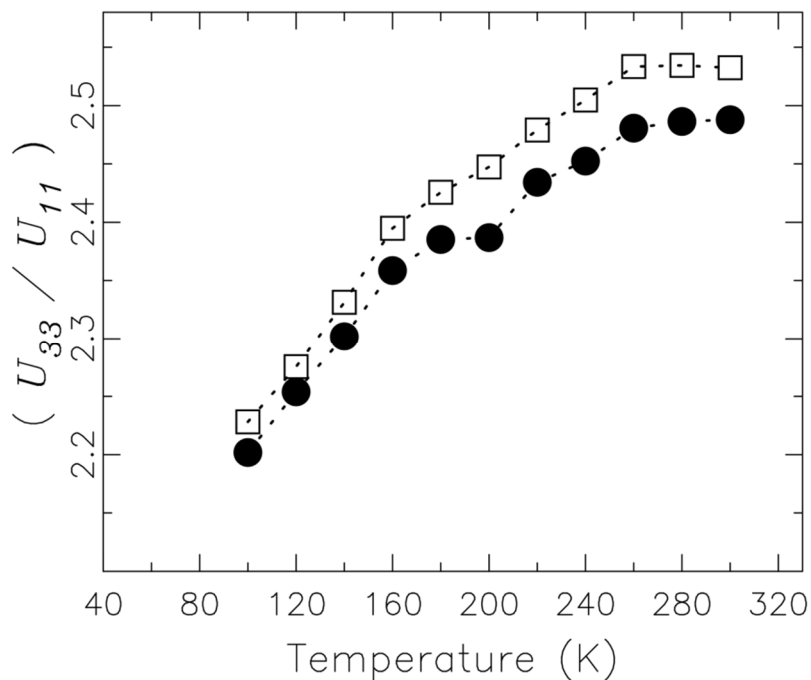


FIG. 5. The ratio of atomic displacement parameters (U_{33} / U_{11}) of zinc as a function of temperature. Solid circles represent long-range refinements. Open squares represent short-range refinements.

3.2 Temperature Dependence of the Axial Ratio c/a

Using the LRR scale, we have also determined the temperature dependence of the lattice parameters a and c . The results are listed

in Table 1. The temperature dependence of the axial ratio c/a is displayed in Fig. 6. A notable observation is that the c/a ratio decreased linearly as the temperature changed from 300 to 100 K.

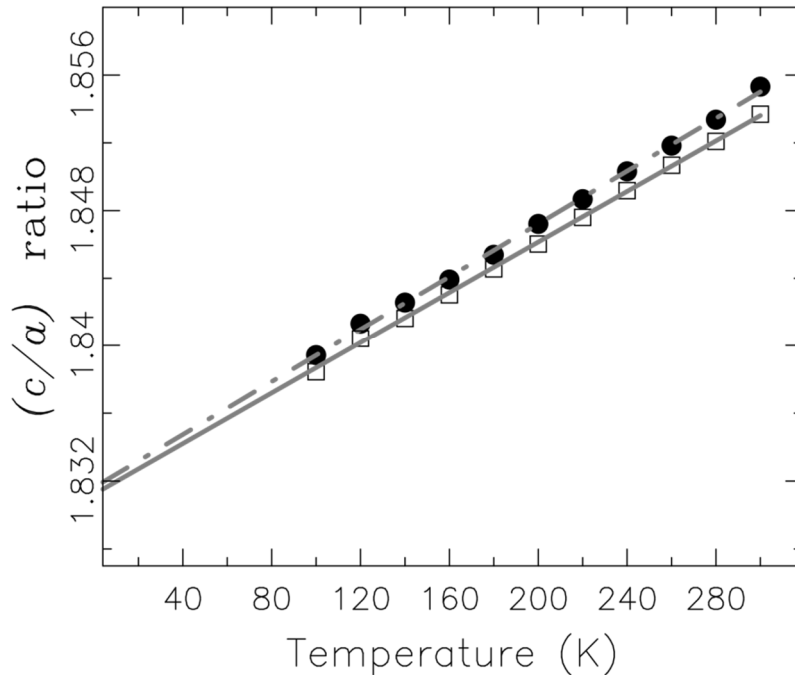


FIG. 6. The ratio of the lattice parameters c/a as a function of temperature. Solid circles stand for long-range refinements and open squares stand for short-range refinements.

This linear behavior is expressed by Eq. (1). At $T = 0$ K, the extrapolated value for c/a is 1.832, which is still large compared to the c/a ratio for an ideal *hcp* structure (1.63). This indicates that the structure anisotropy does not vanish as the temperature approaches absolute zero.

$$[c/a](T)_{LRR} = 1.8316(2) + 7.8(1) \times 10^{-5} \cdot T \quad (1)$$

To study the local order features for the c/a ratio, we performed the SRR scale by fitting the PDF data in the 2-10 Å range. The resulting fit is shown in Fig. 4. The obtained values of c/a from the SRR scale have been compared to the ones obtained from the LRR scale, as demonstrated in Fig. 6. The SRR refinements reveal that the c/a ratio tends to have the same value compared to the LRR refinement as the temperature decreases. Figure 6 shows the obtained axial ratio c/a as a function of temperature for both ranges, LRR and SRR. In this figure, the obtained linear behavior for the c/a ratio from the PDF refinements is expressed by Eqs. (1) and (2), for the LRR and SRR scales, respectively. The extrapolated value at $T = 0$ K is $c/a = 1.832$ in both refinement ranges.

The temperature-dependent PDF refinements conducted for various length scales indicate that there are no significant features for the U_{33} / U_{11}

and c/a ratios at the local level, and they tend to have the same average values. This phenomenon can be attributed to the fact that, regardless of the refinement range (LRR or SRR), the imposed refined model maintains hexagonal symmetry, accompanied by a broad distribution of bond length along the c -direction. This characteristic is reflected in the U_{33} / U_{11} values, resulting in an excellent agreement factor (R_w).

$$[c/a](T)_{SRR} = 1.8312(1) + 7.5(6) \times 10^{-5} \cdot T \quad (2)$$

3.3 Supercell Approach

In the literature, a supercell approach was introduced by Wu *et al.* [24] to investigate the generalized stacking fault energy and surface properties for *hcp* metals. They found adequate convergence concerning the supercell size consisting of twelve layers. This inspired us to adopt a supercell model with a cell size of $1 \times 1 \times 6$. For this supercell model, the z -fraction coordinates for the twelve-layer were refined. The PDF fitting with an excellent agreement factor (R_w) value of 0.045 is shown in Fig. 6. The PDF refinement results using this supercell model are summarized in Table 2. It was observed that the enlargement in the U_{33} value was reduced after including more layers in the PDF refinement and allowing the z -coordinate to vary. The obtained result suggests

the presence of local breaking in *hcp* symmetry along the *c*-direction, as the atoms tend to move off of their ideal sites along the *z*-direction, as was evident in the PDF data, which showed a

wide distribution of the out-of-plane bond (large U_{33} value). This can be reduced by relaxing the layer-to-layer separation distance.

TABLE 2. The results of the PDF refined parameters using a supercell model with a cell size of $1 \times 1 \times 6$ while maintaining the hexagonal symmetry, $U_{11} = 0.01013(4)$ (\AA^2) = $U_{22} \neq U_{33} = 0.01313(1)$ (\AA^2), $U_{12} = 0.5U_{22}$, $U_{13} = U_{23} = 0$. The agreement factor (R_w) value of the refinement is 0.045.

atom	<i>x</i>	<i>y</i>	<i>z</i>
Zn(1)	0.3333	0.6666	0.0435(7)
Zn(2)	0.3333	0.6666	0.5374(6)
Zn(3)	0.3333	0.6666	0.2074(6)
Zn(4)	0.3333	0.6666	0.7123(5)
Zn(5)	0.3333	0.6666	0.3697(4)
Zn(6)	0.3333	0.6666	0.8726(7)
Zn(7)	0.6666	0.3333	0.9564(2)
Zn(8)	0.6666	0.3333	0.4625(3)
Zn(9)	0.6666	0.3333	0.7925(3)
Zn(10)	0.6666	0.3333	0.2876(4)
Zn(11)	0.6666	0.3333	0.6302(5)
Zn(12)	0.6666	0.3333	0.1273(2)

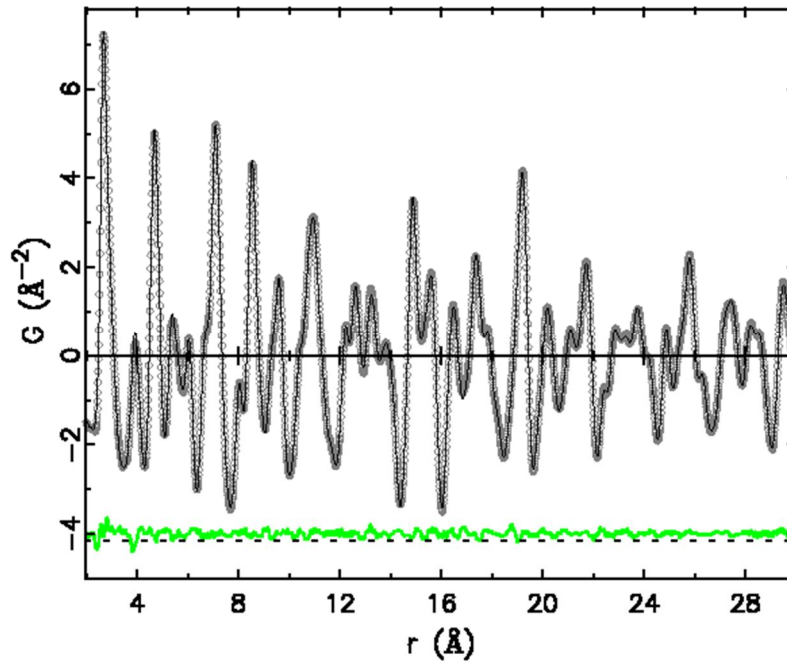


FIG. 6. The experimental $G(r)$ obtained by Fourier transforming the data in (a) (solid dots) and the calculated PDF from a refined supercell model with a cell size of $1 \times 1 \times 6$ (solid line). The difference curve is shown offset below. The black dashed line in the figure is a guide for the eye.

4. Conclusion

The atomic structure of zinc metal is investigated as a function of temperature using the total scattering atomic pair distribution function (PDF) analysis based on X-ray powder diffraction data collected in the temperature range of 100-300 K.

This total scattering study indicates that there is a significant static distortion along the *c*-direction perpendicular to the *ab* plane. This static structural anisotropy in the atomic displacement parameter is still significant at low temperatures, where the thermal motions are reduced (U_{33} / U_{11} value about 2.2 at 100 K). The features of the local structure were investigated using PDF analysis for short-range

refinement (2.0 to 10.0 Å) for different temperatures and compared to long-range refinement (2.0 to 35.0 Å). It was found that there is no significant difference between the results of both refinement ranges, as the hcp model with bond anisotropy ($U_{33} / U_{11} \approx 2.5$) is maintained. The PDF analysis using short range shows that the first crystallographic out-of-plane peak (2.9120 Å) appears to be shorter locally. The obtained c/a ratio is found to reduce linearly as the temperature reduces from 300 to 100 K and extrapolates a value of 1.832 at 0 K. This indicates that the present structure anisotropy

does not vanish as the temperature approaches absolute zero.

Acknowledgments

The PDF data were collected at the 11IDC beamline at the Advanced Photon Source (APS). Use of the APS at Argonne National Laboratory is supported by the U.S. DOE, Office of Science, Office of Basic Energy Sciences, under Contract No. DE-AC02-06CH11357. A. S. Masadeh would like to acknowledge the financial support from the Deanship of Academic Research (DAR) at the University of Jordan.

References

- [1] Nuss, J., Wedig, U., Kirfel, A. and Jansen, M, *Z. Anorg. Allg. Chem.*, 636 (2010) 309.
- [2] Wedig, U., Nuss, H., Nuss, J., Jansen, M., Andrae, D., Paulus, B., Kirfel, A. and Weyrich, W., *Z. Anorg. Allg. Chem.*, 639 (2013) 2036.
- [3] Billinge, S.J.L. and Kanatzidis, M.G., *Chem. Commun.*, 7 (2004) 749.
- [4] Egami, T. and Billinge, S.J.L., "Underneath the Bragg Peaks: Structural Analysis of Complex Materials", 1st Ed. (Pergamon Press, Elsevier, Oxford, England, 2003).
- [5] Chupas, P.J., Qiu, X., Hanson, J.C., Lee, P.L., Grey, C.P. and Billinge, S.J.L., *J. Appl. Crystallogr.*, 36 (2003) 1342.
- [6] Hammersley, A.P., Svenson, S.O., Hanfland, M. and Hauserman, D., *High Pressure Res.*, 14 (1996) 235.
- [7] Juhás, P., Davis, T., Farrow, C.L. and Billinge, S.J.L., *J. Appl. Crystallogr.*, 46 (2013) 560.
- [8] Billinge, S.J.L. and Farrow, C.L., *J. Phys: Condens. Mat.*, 25 (2013) 454202.
- [9] Peterson, P.F., Božin, E.S., Proffen, T. and Billinge, S.J.L., *J. Appl. Crystallogr.*, 36 (2003) 53.
- [10] Masadeh, A.S., *Jordan J. Phys.*, 4 (2011) 79.
- [11] Skinner, L.B., Benmore, C.J. and Parise, J.B., *Nucl. Instrum. Meth. A*, 662 (2012) 61.
- [12] Chupas, P.J., Chapman, K.W. and Lee, P.L., *J. Appl. Crystallogr.*, 40 (2007) 463.
- [13] Proffen, T., Egami, T., Billinge, S.J.L., Cheetham, A.K., Louca, D. and Parise, J.B., *Appl. Phys. A*, 74 (2002) s163.
- [14] Farrow, C.L., Juhás, P., Liu, J., Bryndin, D., Božin, E.S., Bloch, J., Proffen, T. and Billinge, S.J.L., *J. Phys-Condens. Mat.*, 19 (2007) 335219.
- [15] Juhás, P., Farrow, C.L., Yang, X., Knox, K.R. and Billinge, S.J.L., *Acta Crystallogr. A*, 71 (2015) 562.
- [16] Granlund, L., Billinge, S.J.L. and Duxbury, P.M., *Acta Crystallogr. A*, 71 (2015) 392.
- [17] Yang, X., Juhás, P., Farrow, C. and Billinge, S.J.L., *arXiv 1402* (2015) 3163.
- [18] Gilbert, B., Huang, F., Zhang, H., Waychunas, G.A. and Banfield, J.F., *Science*, 305 (2004) 651.
- [19] Neder, R.B. and Korsunskiy, V.I., *J. Phys.-Condens. Mat.*, 17 (2005) S125.
- [20] Kumpf, C., Neder, R.B., Niederdraenk, F., Luczak, P., Stahl, A., Heske, C. et al., *J. Chem. Phys.*, 123 (2005) 224707.
- [21] Masadeh, A.S., Božin, E.S., Farrow, C.L. and Billinge, S.J.L. *Phys. Rev. B*, 76 (2007) 115413.
- [22] Masadeh, A.S., Shatnawi, M.T.M., Adawi, G. and Ren, Y., *Mod. Phys. Lett. B*, 33 (2019) 1950410.
- [23] Merisalo, M. and Larsen, F.K., *Acta Crystallogr. A*, 33 (1977) 351.
- [24] Wu, X., Wang, R. and Wang, S., *Appl. Surf. Sci.*, 256 (2010) 3409.